



CHORUS

This is the accepted manuscript made available via CHORUS. The article has been published as:

Resonant magnetotunneling between normal and ferromagnetic electrodes in relation to the three-terminal spin transport

Z. Yue, M. C. Prestgard, A. Tiwari, and M. E. Raikh

Phys. Rev. B **91**, 195316 — Published 21 May 2015

DOI: [10.1103/PhysRevB.91.195316](https://doi.org/10.1103/PhysRevB.91.195316)

Resonant magneto-tunneling between normal and ferromagnetic electrodes in relation to the three-terminal spin transport

Z. Yue¹, M. C. Prestgard², A. Tiwari², and M. E. Raikh¹

¹*Department of Physics and Astronomy, University of Utah, Salt Lake City, UT 84112, USA*

²*Department of Materials Science and Engineering,
University of Utah, Salt Lake City, Utah 84112, USA*

The recently suggested mechanism [Y. Song and H. Dery, Phys. Rev. Lett. **113**, 047205 (2014)] of the three-terminal spin transport is based on the resonant tunneling of electrons between ferromagnetic and normal electrodes via an impurity. The sensitivity of current to a weak external magnetic field stems from a spin blockade, which, in turn, is enabled by strong on-site repulsion. We demonstrate that this sensitivity exists even in the absence of repulsion when a single-particle description applies. Within this description, we calculate exactly the resonant-tunneling current between the electrodes. The mechanism of magnetoresistance, completely different from the spin blocking, has its origin in the interference of virtual tunneling amplitudes. Spin imbalance in ferromagnetic electrode is responsible for this interference and the resulting coupling of the Zeeman levels. This coupling also affects the current in the correlated regime.

PACS numbers: 72.15.Rn, 72.25.Dc, 75.40.Gb, 73.50.-h, 85.75.-d

I. INTRODUCTION

In the past decade there was a remarkable progress in fabrication of lateral structures which combine ferromagnetic and normal layers and exhibit spin transport. First experimental evidence of spin injection from a ferromagnet into a nonmagnetic material was obtained with the help of four-terminal (4T) technique. This technique was developed in the pioneering papers Refs. 1, 2. It utilizes two ferromagnetic electrodes, injector and detector, coupled to a normal channel. With detector circuit being open, the charge current does not flow between the electrodes. Instead, the current circulating in the injector circuit leads to the voltage buildup between the detector and the normal channel. This nonlocal voltage is suppressed by a weak magnetic field normal to the direction of magnetizations of the electrodes. Such a suppression, called the Hanle effect, reflects the precession of the spin of carriers in course of diffusion between the electrodes. Thus, the characteristic width of the Hanle curve is the inverse spin relaxation time.

More recently, experimental studies of spin injection were carried out using the three-terminal³⁻¹³ (3T) technique. Unlike the 4T technique, in this technique the injector and detector electrodes are combined. The signal measured is the contact voltage between the ferromagnet and the normal channel. Thus, the sensitivity of this signal to the applied magnetic field can be viewed as simply the magnetoresistance of the junction containing ferromagnetic and normal electrodes.

In a number of papers, see e.g. Refs. 4, 9, 12, the sensitivity of the 3T signal to a weak magnetic field is, by analogy to the 4T signal, identified with the spin precession. Namely, it is maintained that the measured signal in the 3T geometry is the sum of two components, one coming from the resistance of the FM contact and the second resulting from the local accumulation of the spins

beneath the ferromagnetic contact.

Experimental results reported in Refs. 3-13 consistently reveal two puzzling features of the 3T magnetoresistance. Unlike the normal Hanle curves, the magnetic field response of the 3T signal shows up for orientations of the external *both* parallel as well as perpendicular to the magnetization of the injector. Moreover, the signs of magnetoresistance are *opposite* for the two field orientations. In addition, the 3T magnetoresistance curves are much broader than the inverse spin-relaxation times measured independently. In general, the basic underlying physics of magnetoresistance in transport between ferromagnetic and normal electrodes constitutes a puzzle. Indeed, even if the portion of a channel under the ferromagnetic electrode accumulates the spin, the normal electrode, acting as a detector, does not “discriminate” between different spin orientations, and, thus, the current should not be sensitive to the spin precession.

Possible resolution of these puzzles was proposed very recently in the theoretical paper Ref. 14 and received some experimental support in the subsequent publications Refs. 15-17. The main idea of Ref. 14 is that the passage of current between the ferromagnet and the normal electrode can be modeled as resonant tunneling via an impurity, see Fig. 1. On the qualitative level, the physics uncovered in Ref. 14 can be explained as follows. When the current flows from normal into ferromagnetic electrodes, the spins of electrons arriving on the impurity do not have a preferential direction. Suppose that the ferromagnet is fully polarized in \uparrow direction. Then electrons arriving with spin \downarrow will never tunnel into the ferromagnet. External magnetic field induces precession of spins of the arriving electrons. Then the electrons, which were “trapped” on the impurity without magnetic field, get a chance to tunnel, unless the field is not parallel to the magnetization. As a result, the current, which did not flow in a zero field, becomes finite. Characteristic value of magnetic field can be estimated by equating the

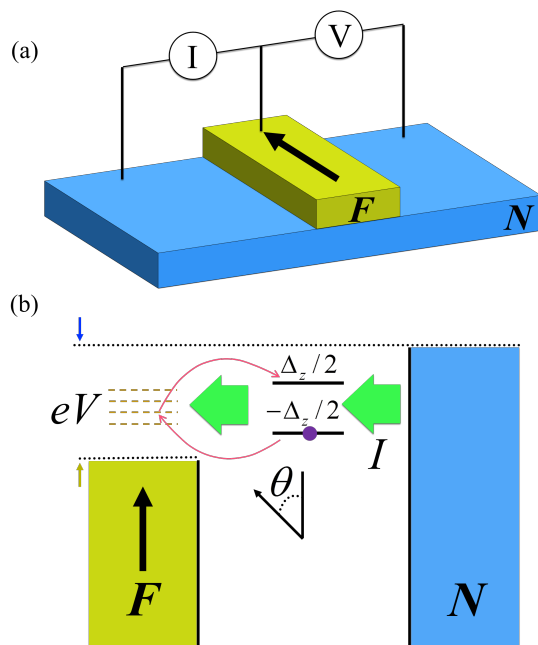


FIG. 1: [Color online] (a) Electrical setup for measuring the spin accumulation within the 3T technique. (b) Energy diagram illustrating the passage of current in (a). The transport is by resonant magnetotunneling between a normal electrode and a ferromagnet. External field, tilted by an angle θ from the direction of magnetization, causes a splitting, Δ_z , of the the impurity level. For non-zero θ two Zeeman levels get coupled via a continuum of the states in a ferromagnet.

period of precession to the waiting time for tunneling. The mechanism is efficient if the spin relaxation rate is smaller than the tunneling rate. Obviously, for the reverse bias, when electrons flow from the ferromagnet this mechanism does not apply.

The key ingredient of the above scenario is a strong repulsion, U , of \uparrow and \downarrow electrons on the impurity. Indeed, if the tunneling of the \downarrow electron is forbidden, then, without the repulsion, the current will be carried by \uparrow electrons, so that there will be no “blockade”.

In the present paper we address a question: whether large U is indeed necessary to induce magnetoresistance. The question is delicate, since, for $U = 0$, the current does not depend on the polarity of bias. Thus, if magnetoresistance is finite for tunneling into a ferromagnet, it should be the same for tunneling into a normal electrode, which is highly non-obvious. On the other hand, for $U = 0$ the current can be calculated exactly. Indeed, resonant tunneling in external field can be viewed as a two-channel resonant tunneling¹⁸ via the Zeeman-split

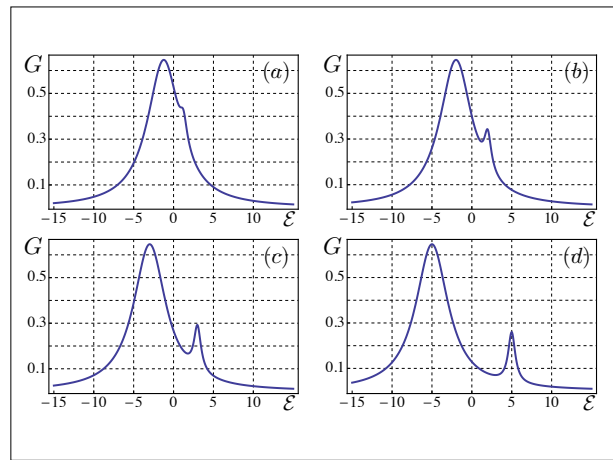


FIG. 2: Differential conductance, $G(\mathcal{E})$, in the units of $e^2/\pi\hbar$ is plotted from Eq. (12) for different dimensionless magnetic fields, in the units Δ_z/Γ_N . (a)-(d) correspond to $\Delta_z/\Gamma_N = 2.5, 4, 6$, and 10 , respectively. All curves are plotted for $\Gamma_F = 2\Gamma_N$ and the orientation of magnetic field, $\theta = 15^\circ$.

levels. Our main analytical result is that magnetoresistance is finite for $U = 0$, and its magnitude is about 50%. The physical origin of the magnetoresistance is the interference of the two transport channels, or, in other words, the coupling of Zeeman levels via a continuum of states in the ferromagnet. We also trace how this coupling affects the current in the regime of correlated transport¹⁴.

The paper is organized as follows. In Sect. II we derive and analyze the expression for non-interacting resonant conductance via two Zeeman levels and, subsequently, for the net resonant current. In Sect. III we study how the coupling of the Zeeman levels via a ferromagnet affects the current in the presence of correlations. Concluding remarks are presented in Sect. IV.

II. MAGNETORESISTANCE IN THE ABSENCE OF COULOMB CORRELATIONS

A. General expression

Within a non-interacting picture we can view the tunneling through a single impurity in a magnetic field as tunneling via two Zeeman-split levels. The non-interacting current-voltage characteristics can be calculated from the tunnel conductance, $G(\mathcal{E})$, as follows

$$I = \int d\mathcal{E} \left[f\left(\mathcal{E} - \frac{V}{2}\right) - f\left(\mathcal{E} + \frac{V}{2}\right) \right] G(\mathcal{E}), \quad (1)$$

where V is the bias, and $f(\mathcal{E})$ is the Fermi distribution.

If the electrodes are normal, the tunneling via each Zeeman level, $\pm\Delta_z/2$, proceeds independently, and $G(\mathcal{E})$ is given by the Breit-Wigner formula

$$G_{\pm}(\mathcal{E}) = \frac{e^2}{\pi\hbar} \left[\frac{\Gamma_L\Gamma_R}{(\mathcal{E} \pm \frac{1}{2}\Delta_z)^2 + \frac{1}{4}(\Gamma_L + \Gamma_R)^2} \right], \quad (2)$$

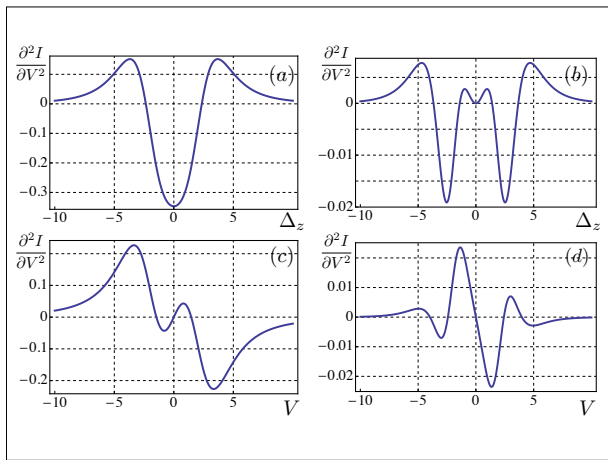


FIG. 3: The second derivative, $\frac{\partial^2 I}{\partial V^2}|_{\theta=\pi/2}$ ((a),(c)) and the difference, $\frac{\partial^2 I}{\partial V^2}|_{\theta=\pi/2} - \frac{\partial^2 I}{\partial V^2}|_{\theta=0}$ ((b),(d)) are plotted from Eqs. (1), (12) versus dimensionless magnetic field, Δ_z/Γ_N , (a) and (b), and versus dimensionless bias, V/Γ_N , (c) and (d). Note, that the unites on the vertical axis are $e^3/\pi\hbar\Gamma_N$. In (a) and (b) the bias is $V = 2\Gamma_N$, while in (c) and (d) the magnetic field is $\Delta_z = 2\Gamma_N$. In all plots $\Gamma_F = 1.5\Gamma_N$, polarization is $p = 1/3$, and temperature is $T = 10\Gamma_N$.

where Γ_L and Γ_R are the widths with respect to tunneling into the left and right electrodes, respectively.

Two tunneling channels are independent because the normal electrodes do not couple the Zeeman levels, since the corresponding spinors are orthogonal to each other. By contrast, a ferromagnetic electrode *does* introduce the coupling between the levels for any orientation of magnetic field except for the field parallel to the magnetization. Indeed, if the angle between the magnetic field and magnetization is θ , the spinors corresponding to the Zeeman levels are

$$\chi_+ = \cos \frac{\theta}{2} \uparrow + \sin \frac{\theta}{2} \downarrow, \quad \chi_- = \sin \frac{\theta}{2} \uparrow - \cos \frac{\theta}{2} \downarrow, \quad (3)$$

where \uparrow and \downarrow are the spin states in the ferromagnet, and the azimuthal angle is set to zero. Denote with Γ_L^\uparrow and Γ_L^\downarrow the widths of the Zeeman levels with respect to tunneling into the ferromagnet for $\theta = 0$. At finite θ , an electron in the state χ_+ can virtually tunnel into the \uparrow -state of the ferromagnet. The amplitude of this tunneling is $\cos \frac{\theta}{2}$. From the \uparrow -state it can then virtually tunnel into χ_- with amplitude $\sin \frac{\theta}{2}$. The electron can also proceed from χ_+ to χ_- via the \downarrow state of the ferromagnet. The corresponding amplitude is $-\sin \frac{\theta}{2} \cos \frac{\theta}{2}$, i.e. it has the opposite sign. As a result, the coupling matrix element between χ_+ and χ_- is equal to $(\Gamma_L^\uparrow - \Gamma_L^\downarrow) \sin \frac{\theta}{2} \cos \frac{\theta}{2}$. It is finite due to the difference in the densities of the intermediate states.

With two Zeeman levels coupled, the tunneling into

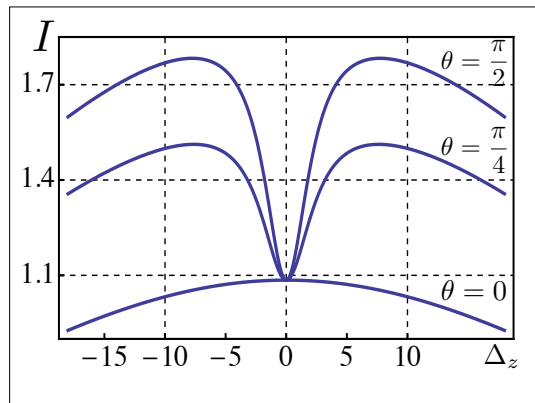


FIG. 4: Resonant-tunneling current (in the units $e\Gamma_N/\pi\hbar$) calculated numerically from Eqs. (1), (12) is plotted versus the dimensionless magnetic field, Δ_z/Γ_N , for different field orientations. In all curves $\Gamma_F = 2\Gamma_N$, the bias is $V = 10\Gamma_N$ and the temperature is $T = 10\Gamma_N$.

the ferromagnet is described by a matrix

$$\hat{\Gamma}^L = \begin{pmatrix} \Gamma_L^\uparrow \cos^2 \frac{\theta}{2} + \Gamma_L^\downarrow \sin^2 \frac{\theta}{2} & (\Gamma_L^\uparrow - \Gamma_L^\downarrow) \cos \frac{\theta}{2} \sin \frac{\theta}{2} \\ (\Gamma_L^\uparrow - \Gamma_L^\downarrow) \cos \frac{\theta}{2} \sin \frac{\theta}{2} & \Gamma_L^\uparrow \sin^2 \frac{\theta}{2} + \Gamma_L^\downarrow \cos^2 \frac{\theta}{2} \end{pmatrix}. \quad (4)$$

This matrix enters into the calculation of the differential conductance, which is given by the matrix generalization of the Landauer formula

$$G(\mathcal{E}) = \frac{e^2}{\pi\hbar} \text{Tr}(\hat{\Gamma}^L \hat{S} \hat{\Gamma}^R \hat{S}^\dagger), \quad (5)$$

where the matrix $\hat{\Gamma}^R$, describing the tunneling into the normal electrode, is diagonal

$$\hat{\Gamma}^R = \Gamma_R \begin{pmatrix} 1 & 0 \\ 0 & 1 \end{pmatrix}. \quad (6)$$

The matrix \hat{S} , which is the Green function in the matrix form, is given by

$$\hat{S} = [\mathcal{E} - \hat{E} + \frac{i}{2}(\hat{\Gamma}^L + \hat{\Gamma}^R)]^{-1}. \quad (7)$$

The matrix \hat{E} in Eq. (7) encodes the energy level positions

$$\hat{E} = \begin{pmatrix} -\frac{1}{2}\Delta_z & 0 \\ 0 & \frac{1}{2}\Delta_z \end{pmatrix}. \quad (8)$$

We will present the result of the evaluating of the matrix product Eq. (5) in the notations of Ref. 14, by denoting with Γ_N (instead of Γ_R) the tunnel width for the normal electrode and introducing the polarization, p , of the ferromagnetic electrode

$$p = \frac{\Gamma_L^\uparrow - \Gamma_L^\downarrow}{2\Gamma_F}, \quad (9)$$

where $\Gamma_F = \frac{1}{2}(\Gamma_L^\uparrow + \Gamma_L^\downarrow)$ is the effective tunneling width for the ferromagnetic electrode, so that

$$\Gamma_L^\uparrow = \Gamma_F(1+p), \quad \Gamma_L^\downarrow = \Gamma_F(1-p). \quad (10)$$

With the new notations, the matrix Eq. (4) assumes a

compact form

$$\hat{\Gamma}^L = \Gamma_F \begin{pmatrix} 1+p \cos \theta & p \sin \theta \\ p \sin \theta & 1-p \cos \theta \end{pmatrix}. \quad (11)$$

The resulting expression for conductance, $G(\mathcal{E})$, reads

$$G(\mathcal{E}) = \frac{2e^2}{\pi\hbar} \Gamma_N \Gamma_F \frac{\mathcal{E}^2 + \frac{1}{4}(\Delta_z^2 + \Gamma_N^2) - \mathcal{E} \Delta_z p \cos \theta + \frac{1}{4}(1-p^2)\Gamma_F(2\Gamma_N + \Gamma_F)}{[\mathcal{E}^2 - \frac{1}{4}(\Delta_z^2 + \Gamma_N^2 + 2\Gamma_F\Gamma_N + (1-p^2)\Gamma_F^2)]^2 + [\mathcal{E}(\Gamma_N + \Gamma_F) - \frac{1}{2}\Gamma_F\Delta_z p \cos \theta]^2}. \quad (12)$$

B. Analysis

Naturally, the dependence $G(\mathcal{E})$ is an even function of \mathcal{E} only for the perpendicular orientation of magnetic field, $\theta = \pi/2$. The asymmetry of $G(\mathcal{E})$ is maximal for the parallel orientation. The asymmetry becomes progressively pronounced with increasing magnetic field, as illustrated in Fig. 2.

The specifics of tunneling from the ferromagnet, as compared to the normal electrode, is that Eq. (12) depends on the orientation of magnetic field. In Ref. 17 the tunneling from cobalt-iron electrode into silicon via an oxide was studied using the inelastic electron tunneling spectroscopy. The curves $\frac{\partial^2 I}{\partial V^2}$ exhibited different behavior for parallel and perpendicular orientations of magnetic field. Motivated by this findings, in Fig. 3 we plot the $\frac{\partial^2 I}{\partial V^2}$ calculated from Eq. (12) for $\theta = \pi/2$ as a function of bias and magnetic field together with the difference of $\frac{\partial^2 I}{\partial V^2}$ for $\theta = \pi/2$ and $\theta = 0$. The value at $\theta = 0$ is finite due to finite polarization $p = 1/3$ of the ferromagnet. All the plots correspond to high temperature $T = 10\Gamma_N$, so that only the magnitude, not the shape, of the curves is T -dependent. It is seen from Fig. 3 that the relative difference of second derivatives is $\sim 10\%$ and exhibits additional structure at small Δ_z and at small bias. Still Fig. 3 cannot account for the results of Ref. 17 where the observed anisotropy was really strong.

An interesting situation unfolds when the bias and temperature are of the same order and are much bigger than the level width. Then the Δ_z -dependence of current, calculated numerically from Eq. (1), exhibits a growth for perpendicular orientation and a minimum for parallel orientation as it is seen in Fig. 4.

C. The net current at large bias

In 3T experiments³⁻¹³ the net current showed the dependence on the magnitude and orientation of magnetic field. It is not obvious whether this dependence is captured by Eqs. (1), (12). For tunneling between normal electrodes, $p = 0$, there should be no magnetoresistance.

Indeed, the expression Eq. (12) can be presented as a sum of two Lorentzians

$$G(\mathcal{E}) = \frac{e^2}{\pi\hbar} \Gamma_N \Gamma_F \times \left[\frac{1}{(\mathcal{E} - \frac{1}{2}\Delta_z)^2 + \frac{(\Gamma_F + \Gamma_N)^2}{4}} + \frac{1}{(\mathcal{E} + \frac{1}{2}\Delta_z)^2 + \frac{(\Gamma_F + \Gamma_N)^2}{4}} \right], \quad (13)$$

so that the Δ_z -dependence disappears upon integration over \mathcal{E} . It turns out that magnetoresistance is nonzero for a finite p . We will present the result for the net current assuming that ferromagnetic electrode is fully polarized, $p = 1$. Then the integration over \mathcal{E} yields

$$I(\Delta_z) = \frac{4e}{\hbar} \Gamma_F \Gamma_N \times \frac{(\Delta_z^2 + \Gamma_N^2 + \Gamma_N \Gamma_F)(\Gamma_N + \Gamma_F) - \Gamma_F \Delta_z^2 \cos^2 \theta}{(\Delta_z^2 + \Gamma_N^2 + 2\Gamma_N \Gamma_F)(\Gamma_N + \Gamma_F)^2 - \Gamma_F \Delta_z^2 \cos^2 \theta}. \quad (14)$$

Eq. (14) is our central result. Sensitivity of the net current to Δ_z originates from the coupling of Zeeman levels via the ferromagnetic electrode [nondiagonal element in matrix Eq. (11)] and, thus, it is most pronounced for $\Gamma_F \gg \Gamma_N$. In this limit Eq. (14) can be simplified to

$$I(\Delta_z) = \frac{4e}{\hbar} \Gamma_N \left(1 - \frac{\Gamma_N \Gamma_F}{\Delta_z^2 \sin^2 \theta + 2\Gamma_N \Gamma_F} \right). \quad (15)$$

The current Eq. (14) is a growing function of magnetic field for all orientations, θ , see Fig. 5. At large Δ_z the current saturates at the value

$$I_\infty = \frac{4e}{\hbar} \Gamma_F \Gamma_N \frac{\Gamma_F \sin^2 \theta + \Gamma_N}{\Gamma_N^2 + 2\Gamma_F \Gamma_N + \Gamma_F^2 \sin^2 \theta}. \quad (16)$$

This saturation value can be understood from the following argument. At large Δ_z the tunneling via upper and lower Zeeman levels get decoupled. The tunnel width of the upper level is $\Gamma_F \cos^2 \frac{\theta}{2} + \frac{1}{2}\Gamma_N$, while the tunnel width of the lower level is $\Gamma_F \sin^2 \frac{\theta}{2} + \frac{1}{2}\Gamma_N$. The sum of the currents corresponding to these widths yields Eq. (16). The

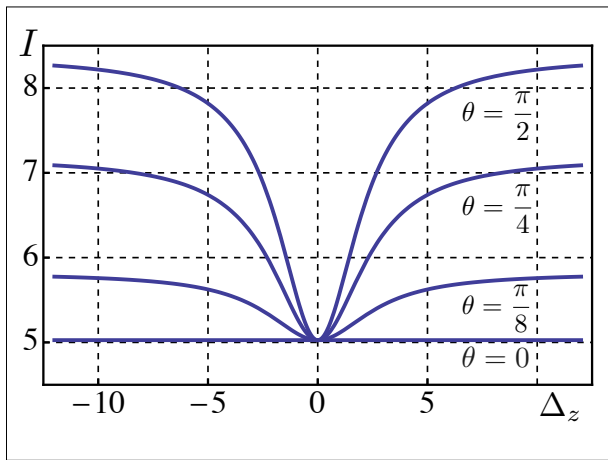


FIG. 5: Resonant current (in the units $e\Gamma_N/\pi\hbar$) in the absence of correlations is plotted from Eq. (14) versus the dimensionless magnetic field, Δ_z/Γ_N , for different field orientations. In all curves $\Gamma_F = 2\Gamma_N$.

same saturation value can be obtained from purely classical consideration, by introducing the probabilities of all four variants of the occupation of the two Zeeman levels and solving the system of master equations for this probabilities.

It is quite nontrivial that in Eq. (15) the characteristic scale of magnetic field, $\Delta_z \sim (\Gamma_F\Gamma_N)^{1/2}$, is much smaller than the level width $\Gamma_F/2$. This suggests that, while the tunneling times for each of the Zeeman levels is Γ_F^{-1} , i.e. short, coupling of these levels via a ferromagnet modifies them in such a way that one of the resulting levels possesses a long lifetime. Similarly to Refs. 18, 21, the origin of this long lifetime can be traced to the complex poles of $G(\mathcal{E})$ in Eq. (12). These poles correspond to the condition: $\det \hat{S}^{-1} = 0$, where the matrix \hat{S} is defined by Eq. (7). The secular equation reads

$$\left[\mathcal{E} - \frac{1}{2}\Delta_z + \frac{i}{2}(\Gamma_N + (1 - \cos\theta)\Gamma_F) \right] \times \left[\mathcal{E} + \frac{1}{2}\Delta_z + \frac{i}{2}(\Gamma_N + (1 + \cos\theta)\Gamma_F) \right] = \left(\frac{i}{2}\Gamma_F \sin\theta \right)^2. \quad (17)$$

The roots of Eq. (17) are

$$\mathcal{E}_{\pm} = \frac{1}{2} \left[i(\Gamma_N + \Gamma_F) \pm \sqrt{\Delta_z^2 - \Gamma_F^2 - 2i\Delta_z\Gamma_F \cos\theta} \right]. \quad (18)$$

For $\Gamma_N \ll \Gamma_F$ and $\Delta_z \ll \Gamma_F$ the imaginary parts of the roots are

$$\text{Im } \mathcal{E}_1 = \frac{1}{2}\Gamma_F, \quad \text{Im } \mathcal{E}_2 = \frac{\Gamma_N}{2} + \frac{\Delta_z^2 \sin^2\theta}{4\Gamma_F}. \quad (19)$$

We see that the time $(\text{Im } \mathcal{E}_2)^{-1}$ is long, and defines the scale $\Delta_z \sim (\Gamma_F\Gamma_N)^{1/2}$ of magnetic field.

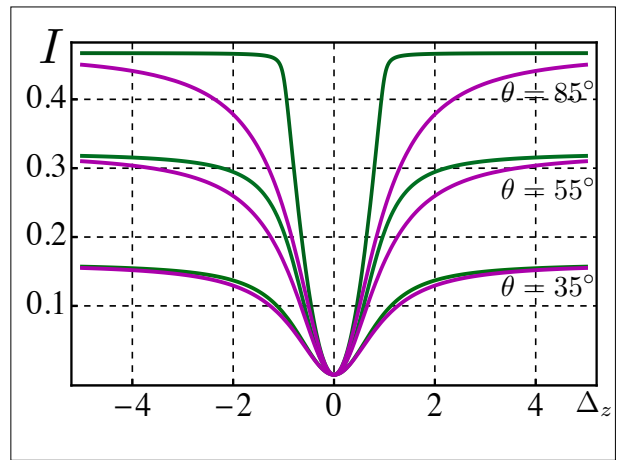


FIG. 6: [Color online] The current from normal into ferromagnetic electrode (in the units $2e\Gamma_F/\hbar$) in the correlated regime is plotted versus dimensionless magnetic field, Δ_z/Γ_F , for different orientations, θ and $\Gamma_N = 8\Gamma_F$. Green curves are plotted from Eq. (31), while the purple curves are plotted from Eq. (32), Ref. 14.

III. CORRELATED TUNNELING

With strong on-site repulsion, U , and the bias, V , exceeding the Kondo temperature, the mechanism of transport is sequential tunneling. The scenario of this sequential tunneling is most simple for $U \gg V$, when the double occupancy of the impurity is forbidden. Then the passage of current, say, from the ferromagnet (F) into normal electrode (N) via impurity (j) proceeds in simple cycles. At the first step, the electron tunnels from F to j , and at the second step, from j to N . The current is inversely proportional to the average duration of the cycle, i.e.

$$I^{F \rightarrow N} = \frac{e}{\tau^{F \rightarrow j} + \tau^{j \rightarrow N}}, \quad (20)$$

where $\tau^{F \rightarrow j}$ and $\tau^{j \rightarrow N}$ are the *average* waiting times for the corresponding tunneling processes. Similarly, the current from N to F is given by

$$I^{N \rightarrow F} = \frac{e}{\tau^{N \rightarrow j} + \tau^{j \rightarrow F}}. \quad (21)$$

For a normal electrode, the time $\tau^{j \rightarrow N}$ is related to $\tau^{N \rightarrow j}$ as²³

$$\tau^{j \rightarrow N} = 2\tau^{N \rightarrow j}, \quad (22)$$

reflecting the fact that tunneling from the electrode onto an empty impurity is possible for both spin directions, while the electron on impurity can tunnel only into the states in the electrode having the same spin direction. If the electrode F was unpolarized, the currents Eqs. (20) and (21) would be given by²³

$$I^{F \rightarrow N} = \frac{e}{2\tau^{j \rightarrow F} + \tau^{j \rightarrow N}}, \quad (23)$$

$$I^{N \rightarrow F} = \frac{e}{\tau^{j \rightarrow F} + 2\tau^{j \rightarrow N}}. \quad (24)$$

For a polarized electrode F the relation $\tau^{j \rightarrow F} = 2\tau^{F \rightarrow j}$ is not valid. In calculating $\tau^{j \rightarrow F}$ one should keep in mind that electron can tunnel into F from both Zeeman levels described by spinors χ_+ , χ_- , Eq. (3), so that

$$\tau^{j \rightarrow F} = \frac{\tau_+^{j \rightarrow F} + \tau_-^{j \rightarrow F}}{2}. \quad (25)$$

In the same way, in calculating $\tau^{F \rightarrow j}$, it should be taken into account that the electron from F can tunnel into both Zeeman levels. The net rate of tunneling is given by

$$(\tau^{F \rightarrow j})^{-1} = (\tau_+^{F \rightarrow j})^{-1} + (\tau_-^{F \rightarrow j})^{-1}. \quad (26)$$

Upon these modifications, the times $\tau^{j \rightarrow F}$ and $\tau^{F \rightarrow j}$ can be very different. Suppose that the polarization is full, $p = 1$, and that the magnetic field is directed along the direction of magnetization. Then for $\tau_+^{j \rightarrow F}$ we have $\tau_+^{j \rightarrow F} = (2\Gamma_F)^{-1}$, while $\tau_-^{j \rightarrow F} = \infty$, reflecting the fact¹⁴ that electron with spin \downarrow cannot tunnel into F , where all spins are \uparrow . For a finite angle, θ , between magnetization and magnetic field this blockade is lifted.

In calculating the tunneling times, it is very important that electron tunnels into F not from pure Zeeman levels, but from the levels coupled via F . This coupling is described by the non-diagonal element of the matrix Eq. (11). Then the corresponding partial times are given by¹⁸

$$\tau_+^{j \rightarrow F} = \tau_+^{F \rightarrow j} = \frac{\hbar}{2\text{Im } \mathcal{E}_+}, \quad (27)$$

$$\tau_-^{j \rightarrow F} = \tau_-^{F \rightarrow j} = \frac{\hbar}{2\text{Im } \mathcal{E}_-}, \quad (28)$$

where \mathcal{E}_+ and \mathcal{E}_- are given by Eq. (18) with $\Gamma_N = 0$.

It can be easily seen from Eq. (18) that the relation

$$\tau_+^{F \rightarrow j} + \tau_-^{F \rightarrow j} = \frac{\hbar}{2\Gamma_F} \quad (29)$$

holds. This, in turn, means that the current $I^{F \rightarrow N}$ is simply equal to $\frac{2e}{\hbar}\Gamma_F\Gamma_N/(2\Gamma_F + \Gamma_N)$, i.e. it does not exhibit any magnetic-field dependence¹⁴. On the other hand, with times given by Eq. (27), the current $I^{N \rightarrow F}$ acquires a non-trivial Δ_z -dependence. Taking into account that

$$\text{Im}\mathcal{E}_\pm = \frac{\Gamma_F}{2} \pm \frac{1}{2} \left[-\frac{1}{2}(\Delta_z^2 - \Gamma_F^2) + \frac{1}{2} \sqrt{(\Delta_z^2 - \Gamma_F^2)^2 + 4\Gamma_F^2 \Delta_z^2 \cos^2 \theta} \right]^{\frac{1}{2}}, \quad (30)$$

we get

$$I^{N \rightarrow F} = \left(\frac{2e}{\hbar} \right) \times \frac{\Gamma_N (\Delta_z^2 + \Gamma_F^2 - \sqrt{(\Delta_z^2 - \Gamma_F^2)^2 + 4\Gamma_F^2 \Delta_z^2 \cos^2 \theta})}{4\Gamma_N \Gamma_F + \Delta_z^2 + \Gamma_F^2 - \sqrt{(\Delta_z^2 - \Gamma_F^2)^2 + 4\Gamma_F^2 \Delta_z^2 \cos^2 \theta}}. \quad (31)$$

It is instructive to compare the result Eq. (31) with corresponding expression from Ref. 14 for $p = 1$, which reads

$$I^{N \rightarrow F} = \left(\frac{2e}{\hbar} \right) \frac{\Gamma_F \Gamma_N \Delta_z^2 \sin^2 \theta}{[(2\Gamma_N + \Gamma_F)\Delta_z^2 + 2\Gamma_F^2 \Gamma_N] - \Gamma_F \Delta_z^2 \cos^2 \theta}. \quad (32)$$

At small θ we can expand the square root in Eq. (31) as

$$\sqrt{(\Delta_z^2 - \Gamma_F^2)^2 + 4\Gamma_F^2 \Delta_z^2 \cos^2 \theta} \approx \Delta_z^2 + \Gamma_F^2 + \frac{2\Delta_z^2 \Gamma_F^2 \theta^2}{\Delta_z^2 + \Gamma_F^2}. \quad (33)$$

It follows from Eq. (33) that the two results coincide at small θ . Otherwise, they are different, see Fig. 6. The difference is most pronounced for $\Gamma_F \ll \Gamma_N$, when the tunneling into F dominates the current. For example, for particular values $\Delta_z = \Gamma_F$ and $\theta = \pi/2$, the current Eq. (31) is two times bigger than $I^{N \rightarrow F}$ given by Eq. (32). The origin of the discrepancy is the form of the Hamiltonian, adopted in Ref. 14, where strong Coulomb repulsion is ascribed to electrons in the states \uparrow and \downarrow . This is permissible only for $\theta = 0$. For nonzero θ , the repulsion takes place between the electrons occupying the eigenstates χ_+ and χ_- , see Eq. (3). Thus, the occupation numbers of χ_+ , χ_- states should enter into on-site repulsion Hamiltonian. In this way the repulsion was incorporated in Refs. 19, 20. Comparison of Eqs. (31) and (32) is presented in Fig. 6.

At large Δ_z the current Eq. (31) saturates at the value

$$I_\infty^{N \rightarrow F} = \frac{2e}{\hbar} \frac{\Gamma_F \Gamma_N \sin^2 \theta}{\Gamma_F \sin^2 \theta + 2\Gamma_N}. \quad (34)$$

In this limit, the coupling between the Zeeman levels is negligible, so that the value $I_\infty^{N \rightarrow F}$ follows from Eq. (23), with $\tau^{N \rightarrow j} = 1/2\Gamma_N$ and $\tau^{j \rightarrow F} = 1/\Gamma_F \sin^2 \theta$. Naturally, the large- Δ_z limit of Eq. (32), in which the coupling of the Zeeman levels is completely neglected, coincides with Eq. (34).

In closing of this Section we present the expression for the current which generalizes Eq. (31) to the case of a finite polarization of the ferromagnetic electrode

$$I^{N \rightarrow F} = \left(\frac{2e}{\hbar} \right) \frac{\Gamma_N (\Delta_z^2 + (2-p^2)\Gamma_F^2 - \sqrt{(\Delta_z^2 - p^2\Gamma_F^2)^2 + 4p^2\Gamma_F^2\Delta_z^2 \cos^2 \theta})}{4\Gamma_N\Gamma_F + \Delta_z^2 + (2-p^2)\Gamma_F^2 - \sqrt{(\Delta_z^2 - p^2\Gamma_F^2)^2 + 4p^2\Gamma_F^2\Delta_z^2 \cos^2 \theta}}. \quad (35)$$

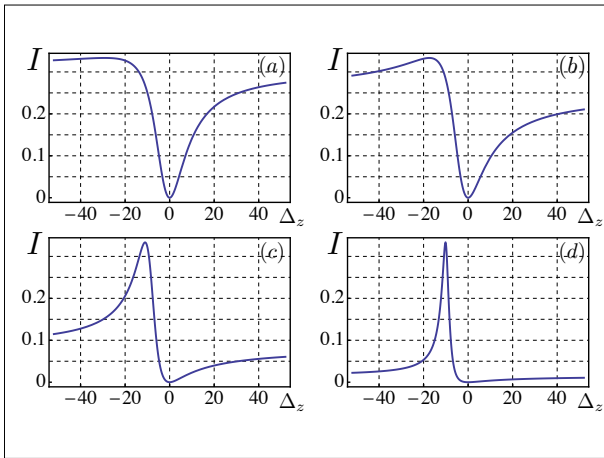


FIG. 7: The effect of pseudomagnetic field on magnetotunneling. The current (in the units $2e\Gamma_F/\hbar$) in the correlated regime is plotted versus dimensionless magnetic field, Δ_z/Γ_F , for orientations $\theta = 70^\circ$ (a), $\theta = 55^\circ$ (b), $\theta = 25^\circ$ (c), and $\theta = 10^\circ$ (d). The plots correspond to $\Gamma_N = \Gamma_F$ and pseudomagnetic field $\Delta_0 = 10\Gamma_F$.

IV. CONCLUDING REMARKS

- Our main physical message is that in resonant magneto-tunneling between the normal electrode and the ferromagnet, the effect of coupling of Zeeman levels via a ferromagnetic electrode affects the current both in correlated and non-correlated regimes. At this point we would like to draw a link to the earlier studies, Refs. 21, 22, where the correlated resonant transport between the *normal* electrodes via a *two-level* system, e.g. two quantum dots in parallel²², was addressed. The authors realized that the current is strongly affected by the coupling between the levels via continuum of the states in the electrodes, and that the rate-equations-based description is invalid due to this coupling. They demonstrated that this coupling gives rise to a strong dependence of current on the energy separation of the levels. In our situation, this separation is simply the Zeeman splitting, Δ_z .

In Refs. 21, 22, the ferromagnet was mimicked by the asymmetry of coupling of the components of the two-level system to the electrodes. In our situation, the source of asymmetry is the angle, θ , between the magnetic field and the magnetization. The effect analogous to “magnetoresistance” was captured in Refs. 21, 22 by numerically solving

the master equations. Our situation, when only one electrode is ferromagnetic, is simpler, which allowed us to get the analytical result Eq. (31) for the correlated current.

- In the correlated regime, the magnetoresistance is present only for one current direction $N \rightarrow F$. Our result Eq. (14) suggests that outside the blocked regime $V > U$, when the current is the same for both voltage polarities, the magnetoresistance is still finite and strong. Probably, this prediction, equal magnetoresistances for both bias polarities for high enough bias, can be tested in 3T spin-transport experiments.
- Except for the papers Refs. 19, 20, 25, 27, the bulk of theoretical studies^{24–26,28–32} of resonant transport between two ferromagnetic electrodes was focused on the low-temperature Kondo regime. As it was pointed in Ref. 25, outside the Kondo regime, in addition to blocking, there is another prominent many-body effect, which results from the polarization of the electrodes and might affect the transport. Namely, the on-site repulsion gives rise to a pseudomagnetic field

$$\Delta_0 = \frac{\Gamma_F}{\pi} \int_{-V/2}^{V/2} d\varepsilon \left(\frac{1}{\varepsilon - U} - \frac{1}{\varepsilon} \right) \quad (36)$$

directed along the magnetization. The structure of Eq. (36) suggests that the underlying mechanism is similar to cotunneling. Incorporating of this field into Eq. (31) is performed by replacing $\Delta_z \cos \theta$ with $\Delta_z \cos \theta + \Delta_0$ and Δ_z^2 with $\Delta_z^2 + \Delta_0^2 + 2\Delta_z\Delta_0 \cos \theta$. The effect of pseudomagnetic field on the shape of magnetoresistance curves is illustrated in Fig. 7. We see that for large enough $\Delta_0 \sim 10\Gamma_F$ the shapes can undergo a dramatic transformation becoming asymmetric and even non-monotonic. Still these shapes do not explain experimental observation that the current grows with Δ_z at $\theta = \pi/2$ and drops with Δ_z at $\theta = 0$. To account for this observation it was assumed in Ref. 14 that, in addition to external field, a strong in-plane hyperfine field is present.

- Throughout the paper we assumed that the impurity level position, \mathcal{E}_0 , is zero. In fact, we required that \mathcal{E}_0 lies within the interval $(-\frac{V}{2}, \frac{V}{2})$, see Fig. 1. For \mathcal{E}_0 lower than $-\frac{V}{2}$ the resonant tunneling is forbidden. It will be allowed again²³ when \mathcal{E}_0 falls into the interval $(-\frac{V}{2} - U, \frac{V}{2} - U)$ (impurity of the “type

B^{''} in the language of Ref. 14). Then the intermediate state for the passage of current will be doubly occupied, and magnetoresistance will be present¹⁴ for $I^{F \rightarrow N}$, but absent for $I^{N \rightarrow F}$. If \mathcal{E}_0 is lower than $-\frac{V}{2}$ but above $\frac{V}{2} - U$, the mechanism of passage of current is cotunneling, i.e. an elastic two-electron process in course of which one electron leaves the impurity to N and another arrives from F . The cotunneling rate, τ_c^{-1} , is given by $\tau_c^{-1} \sim \Gamma_F \Gamma_N / \mathcal{E}_0$, so that the magnitude of current is $I_c = e / \tau_c$. There is a question whether or not the cotunneling current, $I^{F \rightarrow N}$, exhibits the magnetic field dependence. In our opinion it does. Indeed, without the magnetic field and for fully polarized F electrode, the state of the impurity after a single cotunneling act is \uparrow . This forbids the next cotunneling act, so that $I_c = 0$. Finite magnetic field lifts this blockade in the same way as it does for a direct resonant current. We thus expect the magnetoresistance of the

$$\text{form } I^{F \rightarrow N}(\Delta_z) = e \left[\Delta_z^2 \tau_c \sin^2 \theta / (1 + \Delta_z^2 \tau_c^2) \right].$$

- The presence of resonant magneto-tunneling can be confirmed via experimental investigations. The deliberate introduction of atomic-level defects into the tunneling layer can be used to modulate the magneto-tunneling through variations in the defect states present. These variations can be achieved by using defects with different on-site repulsion and investigating the impact of the defect concentration has on the magnetoresistance.

V. ACKNOWLEDGEMENTS

We are grateful to T. Novotný for bringing the paper Ref. 20 to our attention. This work was supported by NSF through MRSEC DMR-1121252.

-
- ¹ M. Johnson and R. H. Silsbee, Phys. Lett. **55**, 1790 (1985).
² F. J. Jedema, A. T. Filip, and B. J. van Wees, Nature (London) **410**, 345 (2001).
³ S. P. Dash, S. Sharma, R. S. Patel, M. P. de Jong, and R. Jansen, Nature **426**, 491 (2009).
⁴ M. Tran, H. Jaffrés, C. Deranlot, J.-M. George, A. Fert, A. Miard, and A. Lemaitre, Phys. Rev. Lett. **102**, 036601 (2009).
⁵ K.-R. Jeon, B.-C. Min, I.-J. Shin, C.-Y. Park, H.-S. Lee, Y.-H. Jo, and S.- C. Shin, Appl. Phys. Lett. **98**, 262102 (2011).
⁶ H. Saito, S. Watanabe, Y. Mineno, S. Sharma, R. Jansen, S. Yuasa, and K. Ando, Solid State Commun. **151**, 1159 (2011).
⁷ N. W. Gray and A. Tiwari, Appl. Phys. Lett. **98**, 102112 (2011).
⁸ R. Jansen, A. M. Deac, H. Saito, and S. Yuasa, Phys. Rev. B **85**, 134420 (2012).
⁹ Y. Aoki, M. Kameno, Y. Ando, E. Shikoh, Y. Suzuki, T. Shinjo, M. Shiraishi, T. Sasaki, T. Oikawa, and T. Suzuki, Phys. Rev. B **86**, 081201(R) (2012).
¹⁰ N. Reyren, M. Bibes, E. Lesne, J. M. George, C. Deranlot, S. Collin, A. Barthèlèmy, and H. Jaffrés, Phys. Rev. Lett. **108**, 186802 (2012).
¹¹ A. Jain, J. C. Rojas-Sanchez, M. Cubukcu, J. Peiro, J. C. LeBreton, E. Prestat, C. Vergnaud, L. Louahadj, C. Portemont, C. Ducruet, V. Baltz, A. Barski, P. Bayle-Guillemaud, L. Vila, J. P. Attané, E. Augendre, G. Desfonds, S. Gambarelli, H. Jaffrés, J. M. George, and M. Jamet, Phys. Rev. Lett. **109**, 106603 (2012).
¹² K. Kasahara, Y. Baba, K. Yamane, Y. Ando, S. Yamada, Y. Hoshi, K. Sawano, M. Miyao, and K. Hamaya, J. Appl. Phys. **111**, 07C503 (2012).
¹³ Y. Pu, J. Beardsley, P. M. Odenthal, A. G. Swartz, R. K. Kawakami, P. C. Hammel, E. Johnston-Halperin, J. Sinova, and J. P. Pelz, Appl. Phys. Lett. **103**, 012402 (2013).
¹⁴ Y. Song and H. Dery, Phys. Rev. Lett. **113**, 047205 (2014).
¹⁵ A. G. Swartz, S. Harashima, Y. Xie, D. Lu, B. Kim, C. Bell, Y. Hikita, and H. Y. Hwang, Appl. Phys. Lett. **105**, 032406 (2014).
¹⁶ O. Txoperena, Y. Song, L. Qing, M. Gobbi, L. E. Hueso, H. Dery, and F. Casanova, Phys. Rev. Lett. **113**, 146601 (2014).
¹⁷ H. N. Tinkey, P. Li, and I. Appelbaum, Appl. Phys. Lett. **104**, 232410 (2014).
¹⁸ T. V. Shahbazyan and M. E. Raikh, Phys. Rev. B **49**, 17123 (1994).
¹⁹ J. N. Pedersen, J. Q. Thomassen, and K. Flensberg, Phys. Rev. B **72**, 045341 (2005).
²⁰ J. N. Pedersen, D. Bohr, A. Wacker, T. Novotný, P. Schmitteckert, and K. Flensberg, Phys. Rev. B **79**, 125403 (2009).
²¹ M. G. Schultz and F. von Oppen, Phys. Rev. B **80**, 033302 (2009).
²² G. Schaller, G. Kießlich, and T. Brandes, Phys. Rev. B **80**, 245107 (2009).
²³ L. I. Glazman and K. A. Matveev, Pisma Zh. Eksp. Teor. Fiz. **48**, 403 (1988) [L. I. Glazman and K. A. Matveev, JETP Lett. **48**, 445 (1988)].
²⁴ J. König and J. Martinek, Phys. Rev. Lett. **90**, 166602 (2003);
²⁵ J. Martinek, Y. Utsumi, H. Imamura, J. Barnaś, S. Maekawa, J. König, and G. Schön, Phys. Rev. Lett. **91**, 127203 (2003).
²⁶ M. Braun, J. König, and J. Martinek, Phys. Rev. B **70**, 195345 (2004).
²⁷ S. Braig and P. W. Brouwer, Phys. Rev. B **71**, 195324 (2005).
²⁸ J. Martinek, M. Sindel, L. Borda, J. Barnaś, J. König, G. Schön, and J. von Delft, Phys. Rev. Lett. **91**, 247202 (2003).
²⁹ M.-S. Choi, D. Sánchez, and R. López, **92**, 056601 (2004).
³⁰ P. Simon, P. S. Cornaglia, D. Feinberg, and C. A. Balseiro, Phys. Rev. B **75**, 045310 (2007).
³¹ S. Lindebaum and J. König, Phys. Rev. B **84**, 235409 (2011).
³² S. Hoffman and Y. Tserkovnyak, arXiv:1412.4663.